Materials & Design 214 (2022) 110413

Contents lists available at ScienceDirect

Materials & Design

journal homepage: www.elsevier.com/locate/matdes

# Mechanisms of stored energy release in silicon carbide materials neutron-irradiated at elevated temperatures ☆

Takaaki Koyanagi *, Hsin Wang, Omer Karakoc, Yutai Katoh

*Materials Science Technology Division, Oak Ridge National Laboratory, Oak Ridge, TN, USA*

## HIGHLIGHTS

- Stored energy release from irradiated SiC composites did not exceed the specific heat capacity, which is promising for accident tolerant fuel applications.
- The model for the energy release behavior derived a total stored energy in irradiated SiC: 425 J/g per 1% swelling.
- The mode concludes that recovery of atomistic defects causing irradiation-induced swelling is the source of the stored energy release.
- The large energy release of 600 J/g during annealing up to 1,273 K was demonstrated for potential energy storage applications.

## GRAPHICAL ABSTRACT

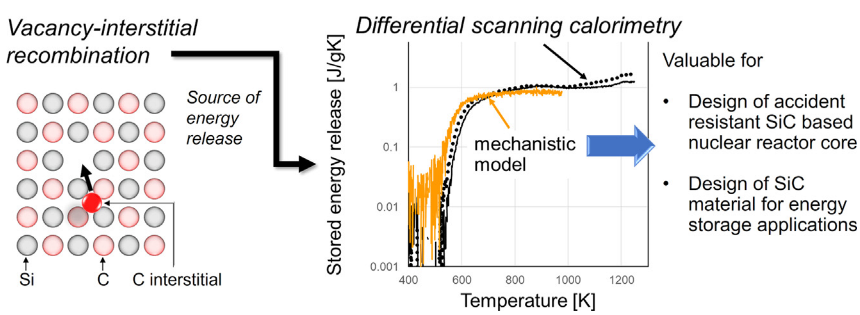


## ARTICLE INFO

*Article history:*
Received 10 September 2021
Revised 17 January 2022
Accepted 18 January 2022
Available online 20 January 2022

*Keywords:*
Stored energy release
Silicon carbide
Neutron irradiation
Differential scanning calorimetry

## ABSTRACT

Understanding the stored energy release behavior of SiC is crucial for the design of SiC-based fuel cladding for light water reactors because stored energy release affects response during accident conditions. Differential scanning calorimetry was used to evaluate the stored energy of monolithic SiC and SiC fiber–reinforced SiC matrix composite variants following neutron irradiation under light water reactor–relevant dose and temperature conditions. The tests were performed at heating rates of 0.5, 3, and 20 K/min up to 1,273 K. The onset temperature of the energy release roughly corresponded to the irradiation temperature, and energy release was delayed as the heating rate increased. The monolithic and composite specimens exhibited similar stored energy release behavior up to $\sim$ 1,000 K, and above that temperature, the energy release depended more on material type. The energy release measured in this study is below the material-specific heat capacity at temperatures below $\sim$1,000 K but exceeds it under certain material and annealing conditions at temperatures above $\sim$1,000 K. The amount of irradiation-induced volumetric swelling of the specimens was an indication of the total stored energy. Based on this observation, the energy release behavior was described by a swelling recovery model.



☆ Notice: This manuscript has been authored by UT-Battelle, LLC, under contract DE-AC05-00OR22725 with the US Department of Energy (DOE). The US government retains and the publisher, by accepting the article for publication, acknowledges that the US government retains a nonexclusive, paid-up, irrevocable, worldwide license to publish or reproduce the published form of this manuscript, or allow others to do so, for US government purposes. DOE will provide public access to these results of federally sponsored research in accordance with the DOE Public Access Plan (http://energy.gov/downloads/doe-public-access-plan).

* Corresponding author at: Oak Ridge National Laboratory, 1 Bethel Valley Road, Oak Ridge, TN 37831-6140, USA.
*E-mail address:* koyanagit@ornl.gov (T. Koyanagi).

https://doi.org/10.1016/j.matdes.2022.110413
0264-1275/© 2022 The Authors. Published by Elsevier Ltd.

## 1. Introduction

Silicon carbide fiber–reinforced SiC matrix (SiC/SiC) composites have been an attractive material option for accident-tolerant fuel cladding for light water reactors (LWRs) and advanced fission reactors since the Fukushima Daiichi nuclear accident because of its inherent advantages of irradiation resistance, high-temperature capabilities, and low neutron absorption [1]. Recent research and development of continuous fiber-reinforced composites have advanced SiC-based composite technologies regarding the tube processing [2,3], understanding of the thermo-mechanical behavior of the component under extreme temperature and loading conditions [4,5], and prediction of material performance by high-fidelity modeling [6,7].

One unaddressed issue is predicting the cladding behavior under specific abnormal conditions [1]. In a loss-of-coolant accident, the properties of SiC/SiC composites are expected to continuously change with increasing temperature, including annealing/recovery of neutron irradiation–induced defects under normal operating conditions and consequential property changes. According to previous irradiation studies on SiC, defect annihilation starts near the irradiation temperature, which triggers the recovery of irradiation-induced swelling and thermal conductivity [8,9]. Such dimensional and thermal property changes affect the performance of SiC-based cladding under accident conditions and could likely improve the response because of thermal conductivity recovery. In addition, defect annihilation results in the release of stored energy that represents the formation energy of the defects. Stored energy release in excess of the material-specific heat would lead to an autocatalytic reaction, which would affect the temperature history of the material system and changes in properties during annealing. These changes would negatively affect the accident resistance of the cladding. Because of the relatively large defect formation energy in SiC [10], understanding its stored energy release behavior is crucial for assessing the accident behavior of SiC-based cladding systems.

Studies of stored energy in neutron-irradiated material stem from the potential danger of stored energy release from graphite, a moderator in nuclear reactors. Fast neutron irradiation causes displacement of atoms from their normal lattice positions into configurations of higher potential energy. As a result, irradiated graphite exhibits higher lattice strain and smaller coherent grain size compared with its pristine condition [11]. When irradiated at temperatures below 423 K, the recombination of Frenkel pairs in graphite is reduced, leading to a buildup of intimate Frenkel pairs that are thought to be the source of stored energy [12]. Annealing of graphite above 473 K allows for recombination of these intimate Frenkel pairs, resulting in a release of energy. If the released energy surpasses the heat capacity of graphite, then a feedback loop is developed, where the excess heat increases the graphite temperature and causes more stored energy release, which increases the graphite temperature (heat excursion) [13]. Although stored energy release is not unique to graphite—because energy release attributed to the recovery of radiation defects could occur in any material—no other type of nuclear ceramics has had an issue with stored energy until recently [10].

In SiC, the accumulation of lattice distortions, an indication of stored energy, is less significant at higher irradiation temperatures since defect recovery processes (i.e., the annihilation of Frenkel pairs) are enhanced in SiC with increasing irradiation temperature [9]. Because SiC was initially proposed for use as a high-temperature structural material (e.g., >1,000 K [14]), stored energy was not considered a risk under accident conditions. Recently, applications for lower irradiation temperatures, including fuel cladding in LWRs operated with coolant at $\sim$ 573 K, have been actively pursued [15], which has increased interest in investigating the stored energy caused by irradiation.

Research pioneers Primak et al. [16] found no evidence of catastrophic stored energy release from irradiated SiC, probably because of the relatively low neutron fluence of $\sim 4 \times 10^{23}$n/m$^2$ (E > 75 eV). In 2019, Snead et al. [10] found a massive energy release of 1,390 J/g upon annealing to 973 K from SiC neutron-irradiated at $\sim$ 333 K to a high neutron fluence of $5 \times 10^{24}$n/m$^2$ (E > 0.1 MeV). The amount of energy released was comparable to that released by nuclear graphite, and the stored energy release exceeded the specific heat in some irradiation conditions. The findings gave rise to concerns about the performance of SiC-based cladding under loss-of-coolant–accident conditions, which could heat the cladding rapidly. Fundamentals of irradiation-induced damages in SiC continued to be explored, and in-depth analysis of the chemical disordering and atomistic defects was conducted [17–19]. Recovery of such radiation damage during annealing is considered a source of the stored energy release [10].

To better understand stored energy release, this study conducted experimental investigations of energy release from irradiated SiC variants under different heating rates by differential scanning calorimetry (DSC). The DSC technique has demonstrated its use for elucidating mechanisms of recovery of defects and disorder during annealing and consequently gained insights to aid material design [20–22]. In this study, the irradiation temperature was relevant to LWR operating conditions; monolithic and composite materials were both tested, which was not the case for the previous studies [10,16]. A mechanistic model of the energy release behavior was developed based on the relationships between stored energy and irradiation-induced swelling.

The DSC experiment was conducted up to 1,273 K, which is relatively low for the accident conditions. Currently, DSC testing at extremely high temperatures requires finding a proper specimen pan that is chemically compatible with SiC specimens and has adequate thermal properties for an accurate measurement of heat capacity. In Section 4, the linear relationship between the rate of energy release and swelling recovery is shown to be useful in predicting energy release at extreme temperatures since a dilatometry method, used for measurement of swelling recovery, was feasible up to 2,273 K [23].

This is the first comprehensive study addressing the stored energy release of SiC for LWR applications. The model for energy release behavior of irradiated SiC is unique: it was developed based on recovery of the radiation-induced swelling, and it derived a total energy stored in irradiated SiC. The model is valuable for design of SiC-based nuclear reactor core structures resistant to accident conditions. Furthermore, the potential of irradiated SiC as an energy storage material is demonstrated because of the large energy release observed.

## 2. Experimental

Four types of SiC variants were tested in this study: two types of monolithic SiC and two types of SiC/SiC composites. Polycrystalline, chemical-vapor-deposited (CVD) β-SiC monoliths were obtained from Dow Chemical Co. (DC) and CoorsTek (CT). Both materials were a high-resistivity grade with a nominal purity of > 99.9995%. The specimens were 6 mm in diameter and 0.5 mm thick. The SiC/SiC composite materials were fabricated by Rolls-Royce High Temperature Composites Inc. (lot number 13C-529). The SiC matrix was infiltrated into a two-dimensional satin-weave fabric by chemical vapor infiltration (CVI). The fiber type was either Hi-Nicalon Type S (HNS) or Tyranno SA3 (SA3) SiC. Both composites had a pyrolytic carbon (PyC) interphase between the fiber and the matrix. The estimated fiber volume fraction was ~ 40%. The SiC/SiC composite plates were machined into bar specimens with dimensions of 25 × 2.8 × 1 mm. The monolithic and composite specimens were machined using a diamond saw and wheel. A 600–800 grit diamond tool was used to create a smooth surface finish. The estimated fiber volume fraction and porosity were ~ 40% and 8–16%, respectively.

Neutron irradiation was conducted in the High Flux Isotope Reactor at Oak Ridge National Laboratory (ORNL). The nominal neutron dose ranged from 2.0 to 11.8 × $10^{25}$n/m$^2$ (E > 0.1 MeV), equivalent to 2.0–11.8 displacements per atom (dpa), assuming that 1 × $10^{25}$n/m$^2$ (E > 0.1 MeV) corresponds to 1 dpa [9]. The damage rate was ~ 1 × $10^{-6}$ dpa/s. The irradiation temperature was 510–880 K. Temperature was experimentally determined by post-irradiation measurement of the length change of passive SiC temperature monitors using a Netzsch DIL 402CD dilatometer since swelling of SiC starts to recover at irradiation temperatures [8]. The irradiation temperatures determined were considered to be nominal irradiation temperatures because the temperatures of the monitors and the specimens could be different, especially for the CVD SiC specimens, based on the thermal modeling of irradiation temperature by ANSYS finite element analysis. The error in temperature determination by data analysis was 10–15 K. The diameters or lengths of unirradiated and irradiated specimens were also obtained using a micrometer with a precision of < 1 μm, which measured length change resulting from irradiation with an error of approximately < 0.03%.

Stored energy in the irradiated specimens was measured in a 99.999% argon atmosphere using a Netzsch DSC 404F1 Thermal Analyzer. The SiC/SiC composite bars were cut into ~ 5 mm lengths before measurement, whereas the CVD monolithic SiC discs were tested without machining. A four-step process to determine the stored energy was used with a sapphire standard following ASTM E1269-11 [24]: (1) the system baseline was obtained by placing empty Pt/Rh pans in the reference and sample positions (at least two baseline runs were made to ensure repeatability); (2) the reference signal was obtained by placing a sapphire standard in the sample pan; (3) specimen evaluation was conducted by placing an irradiated SiC sample in the sample pan; and (4) the irradiated sample was analyzed via DSC again (acting as the specimen baseline). The use of repeat DSC analysis as the baseline depends on there being no additional energy release on the second analysis, and this was supported by the experimental observations. This study defines stored energy release as a difference in the specific heat capacity measured during the first and second heating runs because of the instability of the temperature control at the beginning of cooling. This study used three heating rates of 0.5, 3, and 20 K/min. The cooling rate was set at 20 K/min. The maximum test temperature ranged from 673 to 1,273 K. At the maximum temperature, isothermal holding for at least 30 min was conducted. In addition to measurements on a range of specimens to obtain stored energy release data, an isothermal run was also performed (specimen ID CTA8) to gather input parameters for the model.

In DSC, specific heat capacity ($C_p$) is only sensitive to composition. In other words, $C_p$ of SiC is not affected by different microstructures as long as the composition is the same. For the SiC/SiC composites, porosity in the SiC matrix affects the global composition (fraction of fiber vs. matrix). However, the effects on $C_p$ are insignificant considering the limited volume of C interphase and secondary C phases in fiber (<5 vol%). Therefore, $C_p$ before release of stored energy and after recovery was not affected by sample to sample variations and microscopic inhomogeneity. Therefore, differences in the apparent $C_p$ during annealing are dominantly caused by differences in stored energy release attributed to recovery of radiation defects. It was confirmed that there was no notable reaction among the specimens and the Pt/Rh pan after the measurement. In this study, the effects of potential trace $O_2$ are likely insignificant. Under temperatures below 1,273 K, oxidation of β-SiC is passive regardless of $O_2$ partial pressure [25]. A rate of mass change by the passive oxidation was only − 0.29 mg cm$^{-2}$h$^{-1}$, even at 1,530 K [25]. Additionally, $H_2$ and its isotopes are expected to have an insignificant effect in the DSC experiment, considering extremely low permeability of $H_2$ into SiC [26] and limited H transmutation (3 appm/dpa) [27].

The polished cross-sections of the unirradiated composites were characterized using a Hitachi 4800S scanning electron microscope (SEM). Transmission electron microscopy (TEM) observation of the unirradiated CVD SiC was also conducted using a JEOL JEM2100F with a TEM mode operated at 200 kV. The TEM specimens were prepared using the FEI Quanta 3D 200i Dual Beam SEM/focused ion beam operated at 30 kV for rough milling and 2 and 5 kV for final thinning.

## 3. Results

Both the DC and CT CVD SiC ceramics were polycrystalline β-SiC variants with approximate grain sizes (the equivalent circle diameter of the grain) ranging from 1 to 50 μm (~5 μm on average). Electron backscatter diffraction analysis in an SEM found moderate or no grain texture in the specimens (results not shown here). The notable difference between the specimens was the microstructure of the grain interior. The SiC grains of the DC CVD SiC contained some stacking faults (Fig. 1a). The CT CVD SiC had a significantly higher number density of stacking faults, as shown in Fig. 1b. The streak intensity appearing in the selected area diffraction pattern also indicated significant faulting.

Polished cross-sections of the as-fabricated SiC/SiC composite specimens are shown in Fig. 2. The typical microstructural features of CVI SiC/SiC composites include pores in the matrix and the PyC interphase. The thickness of the PyC interphase ranged from 50 to 160 nm for the HNS-SiC/SiC composite and from 200 to 350 nm for the SA3-SiC/SiC composite. The backscattered electron imaging did not indicate any impurities in the matrix regions. The estimated porosity was 15% for both composites.

Table 1 summarizes the specimen matrices, irradiation conditions, DSC parameters, and results. An example of the DSC curves for heating and cooling rates of 20 K/min for irradiated DC CVD SiC is shown in Fig. 3. The specific heat capacity during the heating in the first run appears to be lower than during the cooling because of the energy release. The second heating and cooling curves are almost identical to the cooling curve of the first run, indicating no additional energy release during the second run.

Fig. 4 shows stored energy release curves of the irradiated CVD SiC and SiC/SiC composites under the DSC experiment with a heating rate of 20 K/min. The irradiation temperatures were 510–520 K or 880 K. The irradiation damage was ~ 2 dpa for the CVD SiC and 11.8 dpa for the SiC/SiC composites. The graph also shows the reference DSC curves obtained from the second DSC run of the irradiated specimens. The reference curves correspond to the specific heat capacity of pure SiC reported by Snead et al. [9]. The reference specific heat capacity of the tested CVD SiC specimens stayed within 5% difference from the literature value in the whole test temperature range, indicating reproductivity of the test data and a homogeneity of the test specimens attributed to the high-purity.

In the cases of irradiation at 510–520 K, the CVD SiC and SiC/SiC composites exhibited similar energy release behavior up to ~ 1,000 K; the onset of energy release corresponds to around 600 K, slightly above the nominal irradiation temperature. At > 1,000 K, the energy release behavior depended more on the material type than on the temperature. The energy release started around the irradiation temperature in the case of irradiation at 880 K. It is worth mentioning that the stored energy release of

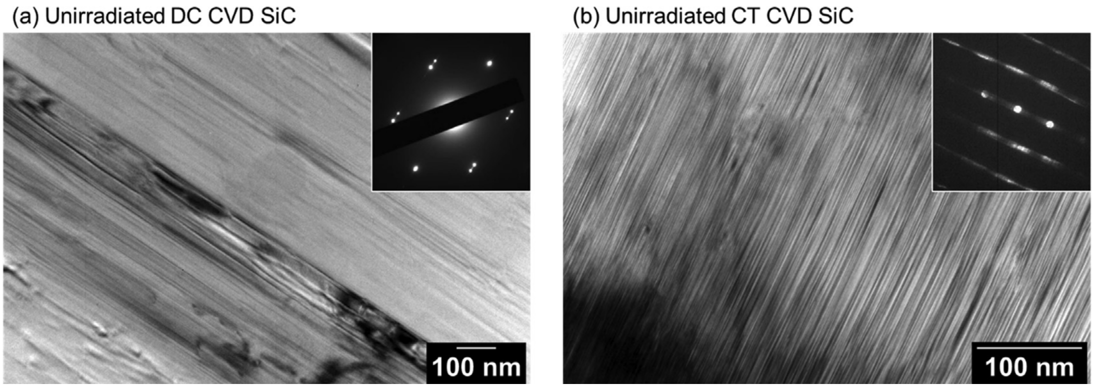


**Fig. 1.** TEM bright field micrographs of as-fabricated (a) DC and (b) CT CVD SiC. The images were taken from the near (1 1 0) zone axis. The inset selected-area diffraction patterns show diffuse streaks indicating (a) moderate-density stacking faults in DC CVD SiC and (b) high-density stacking faults in CT CVD SiC.

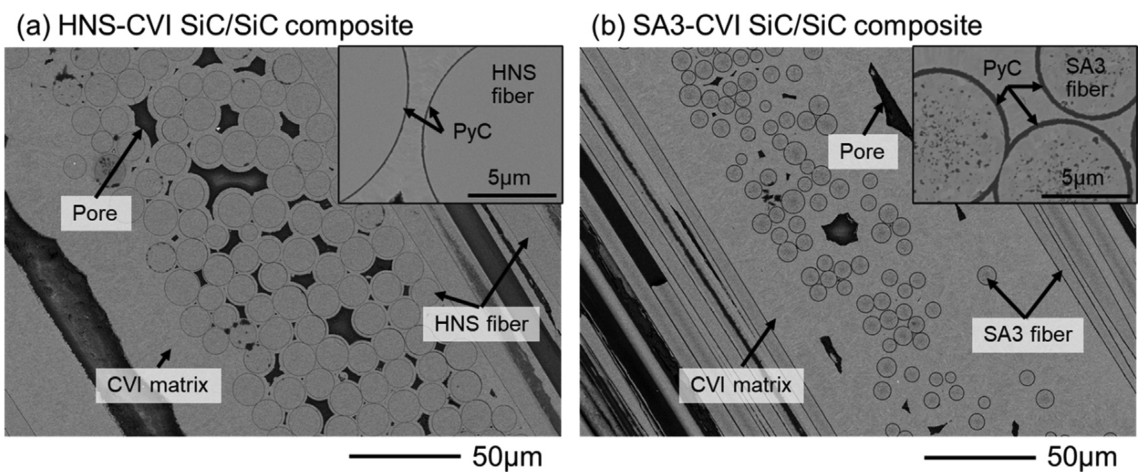


**Fig. 2.** Typical cross-sectional backscattered electron images of unirradiated SiC/SiC composites: (a) HNS-CVI SiC/SiC composite and (b) SA3-CVI SiC/SiC composite.

the SiC materials was below the specific heat capacity at temperatures up to 1,273 K, suggesting no autocatalytic reaction.

Fig. 5 shows how the energy release behavior of irradiated CVD SiC was affected by the heating rate of the DSC run. The onset temperature of energy release of both the DC and the CT CVD SiC was delayed from 0.5 to 20 K/min as the heating rate increased. The increase in heating rate also caused a more gradual energy release around the onset temperature. These trends are understandable; when heating is fast, defects do not have sufficient time to recover, and thus there is less energy release at the beginning. The effects of the heating rate on the onset temperature of energy release appeared similar between the DC and CT CVD SiC. Another result is that the energy release exceeded the specific heat capacity under certain conditions (DC CVD SiC, heating rate of 3 K/min, tempera-

**Table 1**
Summary of test specimens, irradiation conditions, parameters, and results of DSC experiments and irradiation-induced volume changes.

| Specimens | | Irradiation conditions | | DSC conditions | | | Results | | |
|---|---|---|---|---|---|---|---|---|---|
| Material type | Specimen ID | Irradiation temperature (K) | Neutron damage (dpa) | Heating rate (K/min) | Max. test temperature (K) | Holding time (min) | Stored energy up to 973 K (J/g) | Stored energy up to 1,273 K (J/g) | Volumetric swelling (as-irradiated) (%) |
| DC CVD SiC | RHA1 | 510 | 2.0 | 20 | 973 | 30 | 227 | Not tested | 1.9 |
| | RHA2 | 510 | 2.0 | 20 | 973 | 30 | 242 | Not tested | 2.2 |
| | RHA5 | 880 | 2.2 | 20 | 1,273 | 30 | 1.1 | 88 | 0.9 |
| | RHA4 | 510 | 2.0 | 3 | 1,273 | 30 | 336 | 667 | 2.5 |
| | RHA3 | 510 | 2.0 | 3 | 973 | 30 | 462 | Not tested | 2.1 |
| | CVD 5 | 510 | 2.0 | 0.5 | 973 | 30 | 289 | Not tested | 2.4 |
| CT CVD SiC | CTA8 | 510 | 2.0 | 20 | 473 | 180 | Not available | Not tested | 2.1 |
| | CTA5 | 510 | 2.0 | 20 | 1,273 | 30 | 267 | 539 | 2.3 |
| | CTA7 | 510 | 2.0 | 3 | 1,273 | 30 | 303 | 600 | 2.1 |
| | CTA2 | 510 | 2.0 | 0.5 | 973 | 30 | 255 | Not tested | Not available |
| HNS-CVI SiC/SiC | A28-1 | 520 | 11.8 | 20 | 1,273 | 30 | 171 | 377 | 1.7 |
| | A28-2 | 520 | 11.8 | 20 | 1,273 | 30 | 176 | 393 | 1.7 |
| SA3-CVI SiC/SiC | B46-1 | 520 | 11.8 | 20 | 1,273 | 30 | 219 | 446 | 1.9 |
| | B46-2 | 520 | 11.8 | 20 | 1,273 | 30 | 201 | 419 | 1.9 |

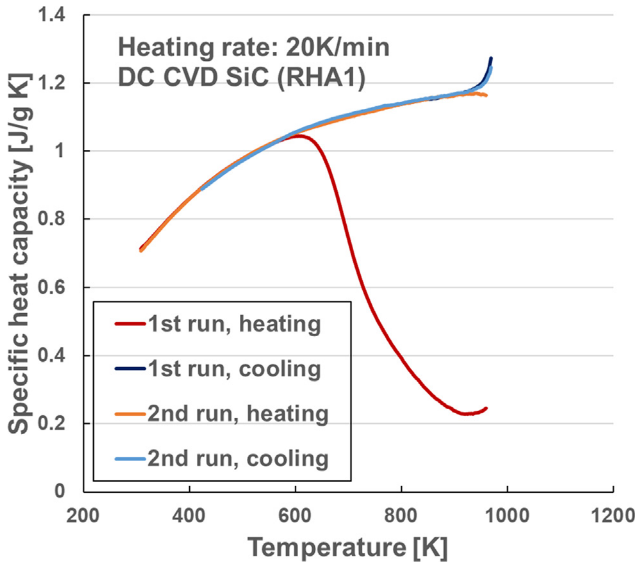


**Fig. 3.** Specific heat capacity measurements of irradiated DC CVD SiC during first and second runs with a heating and cooling rate of 20 K/min. The difference between the first and second heating runs is defined as the stored energy release caused by recovery of the radiation defects.

ture range of > 1,100 K). Even for the other cases, the energy released was very close to the specific heat capacity at > 800 K (the difference was within 10% of the specific heat capacity). This finding indicates that annealing of SiC irradiated at ~ 500 K potentially leads to an autocatalytic reaction, depending on the application.

## 4. Discussion

### *4.1. Modeling energy release behavior*

Total stored energy—the integration of energy released during annealing—is correlated with irradiation-induced volumetric swelling of CVD SiC and SiC/SiC composites, as shown in Fig. 6. The irradiation temperature range was 510–520 K. At these temperatures, SiC does not undergo amorphization by irradiation, and radiation defects cause lattice expansion that results in volumetric swelling [9]. The reported results from CVD SiC irradiated at ~ 330 K up to 0.5 dpa [10], during which swelling was also caused by lattice expansion, are also presented for comparison. For the case of the lower irradiation temperature, a linear correlation between stored energy and swelling was reported, suggesting that swelling was an indication of energy stored in the SiC material [10]. This was the case for the higher irradiation temperature in this study compared with the lower temperature in the work by Snead et al. [10]. The energy release proportionally increases with increasing swelling for annealing up to 973 K. The heating rate and material variation do not appear to have vital effects on the swelling dependence. We consider the stored energy–swelling relationship is key to modeling the release behavior.

The DSC experiments on the SiC variants under different heating rates showed the limited effects of the material type on the energy release behavior up to ~ 973 K (Fig. 4 and Fig. 5), which suggests that the energy release behavior is intrinsic to SiC. Herein, we attempt to model the energy release curves at the low-temperature regime. The key assumption in building a mechanistic model is a linear correlation between the energy released ($R$ [J/g]) and the swelling recovered ($\Delta S$ [no unit]) during isothermal annealing at a temperature ($T$ [K]) for a time duration ($t$ [s]).

$$R(T,t) = k\Delta S \tag{1}$$

where $k$ is a stored energy–swelling conversion constant in J/g. This equation is based on the linear correlation between the stored energy and swelling in Fig. 6 and is consistent with the trend lines which could be drawn by a linear fit with an intercept at the origin. The similarity in the energy release and swelling recovery is also shown in Fig. 4; the energy release initiated around the nominal irradiation temperature as swelling recovered during annealing of SiC [8]. To further validate the assumption, a direct comparison of the energy release and swelling recovery was conducted. The swelling recovery of DC CVD SiC was investigated using a dilatometer (Fig. 7a), and then the rate of recovery from the swelling was converted to an energy release rate according to Eq. (1) and compared with the DSC results. Note that the heating rate of

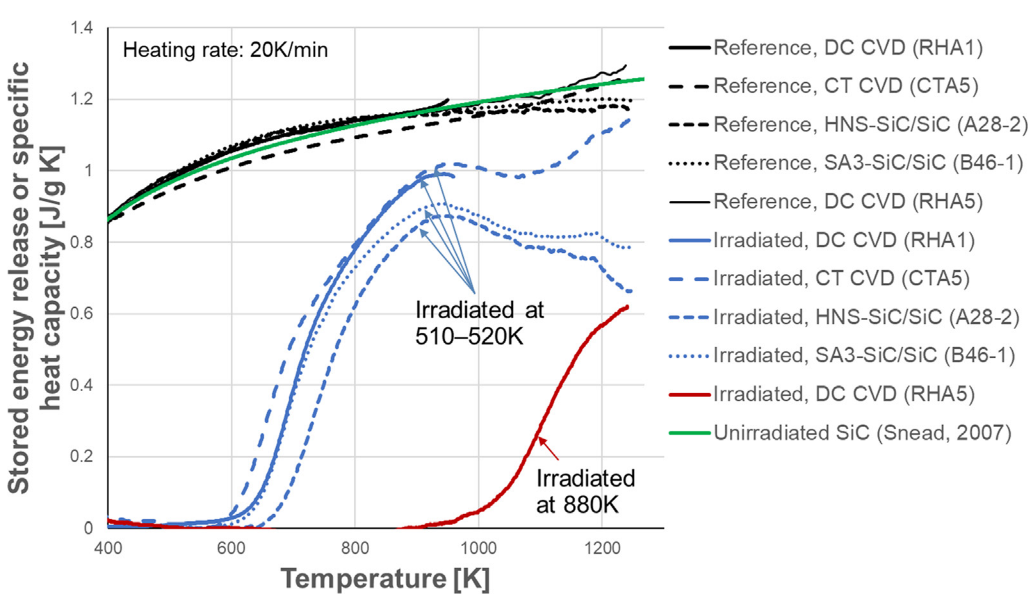


**Fig. 4.** Stored energy release curves of irradiated CVD SiC and SiC/SiC composites (blue and red lines) and the reference DSC curves (black lines) obtained from the second DSC runs. The reference curve (solid green line) corresponds to the specific heat capacity of pure SiC [9]. Measurements were performed at a 20 K/min heating rate. The irradiation temperature was ~ 500 or 880 K. (For interpretation of the references to color in this figure legend, the reader is referred to the web version of this article.)

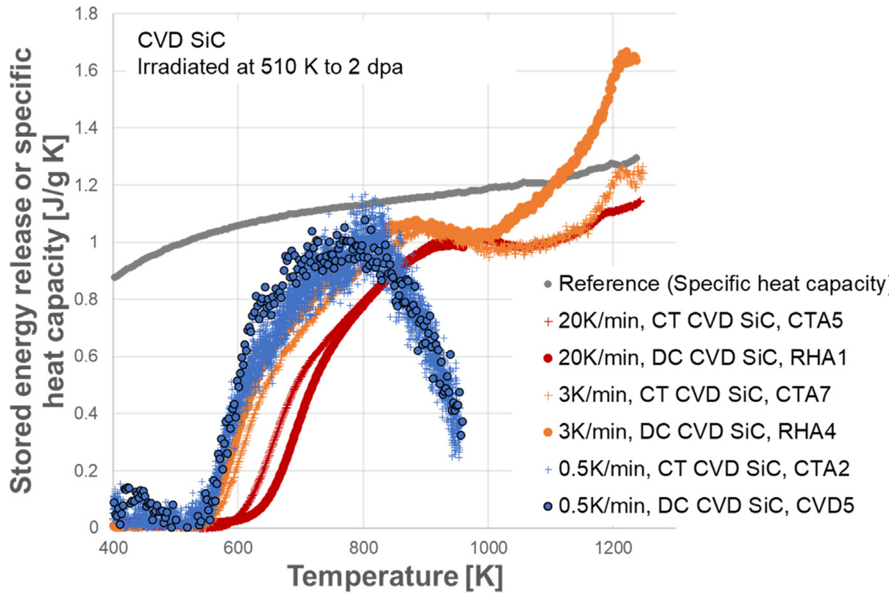


**Fig. 5.** Stored energy release behavior of irradiated CVD SiC materials with heating rates of 0.5, 3, and 20 K/min. The representative reference curve corresponding to the specific heat capacity is also presented.

the dilatometry and DSC experiments was 3 K/min. The energy release model describes well the experimental data when $k$ = 4.25 $\times$ 10$^4$ (J/g) is assigned as shown in Fig. 7b. This value indicates a total stored energy of 425 J/g per 1% of volumetric swelling. This stored energy–swelling conversion is assumed to be insensitive to heating rate.

As the next step of the model development, the time and temperature dependences of swelling recovery ($\Delta S$) were formulated. Although previous studies of the kinetics of SiC swelling recovery have identified the apparent activation energies [28–30], a complete formula of time- and temperature-dependent swelling recovery is not available. In this study, the following equation was used to describe the swelling recovery.

$$\Delta S(T,t) = [S_0 - S_{sat}(T)]\left\{1 - \exp\left[-\frac{t}{\tau(T)}\right]\right\}, \quad (2)$$

where $S_0$, $S_{sat}$, and $\tau$ denote initial swelling (no unit), saturation swelling after isothermal annealing for infinite time (no unit), and lifetime of swelling recovery (in seconds), respectively. When an irradiated SiC specimen is subjected to isothermal annealing at $T$, the swelling recovers to the saturation value ($S_{sat}(T)$). This process is expressed by $S_0 - S_{sat}(T)$. The saturation value upon annealing is considered to be identical to the saturation value of swelling during irradiation at the temperature. CVD SiC and CVI SiC/SiC composites undergo transitional swelling at intermediate temperatures, from approximately 420 to 1,300 K, and the swelling saturates at $\sim$ 2 dpa at a value that depends on and negatively correlates with the irradiation temperature [9,31]. Temperature and dose dependence of irradiation-induced swelling rate in SiC (in dpa$^{-1}$) is described by the following equation [32]:

$$\frac{dS}{d\gamma} = k_s\gamma^{-\frac{1}{3}}exp(-\frac{\gamma}{\gamma_C}) \quad (3)$$

where $S$ denotes swelling (no unit), $\gamma$ denotes the displacement damage dose (dpa), $k_s$ denotes the rate constant ($dpa^{-\frac{2}{3}}$), and $\gamma_C$ denotes the characteristic dose in dpa for swelling saturation. This study uses $\gamma_C$ of 0.2 dpa at < 873 K and 0.3 dap at 873–973 K according to the dose dependence of swelling of SiC [9,32]. The dose dependence exponent –1/3 is for self-interstitial atoms forming two-dimensional clusters (i.e., extrinsic dislocation loops). The rate constant $k_s$ is negatively proportional to irradiation temperature to describe the saturation swelling of SiC linearly decreasing as irradiation temperature increases in the temperature range 473–1073 K [9]. The following equation for $k_s$ reproduces the reported experimental data [32]:

$k_s$ = A $T$ + B (4)

in which A is 1.01 $\times$ 10$^{-4}$ $K^{-1}dpa^{-\frac{2}{3}}$ and B is 1.12 $\times$ 10$^{-1}$ $dpa^{-\frac{2}{3}}$. The equations (3) and (4) provide $S_{sat}(T)$ at different temperatures.

The second part of Eq. (2), $1 - \exp\left[-\frac{t}{\tau(T)}\right]$, expresses an exponential decay of the swelling recovery as a function of time, assuming a thermally activated process. The temperature-dependent rate constant, $\tau(T)$ in seconds, expresses the decay behavior and a lifetime of defect recombination. Exponential decay of swelling recovery at the beginning of annealing has been observed by dilatometry of irradiated SiC [33]. The key parameter $\tau(T)$ can be expressed by the Arrhenius expression [30],

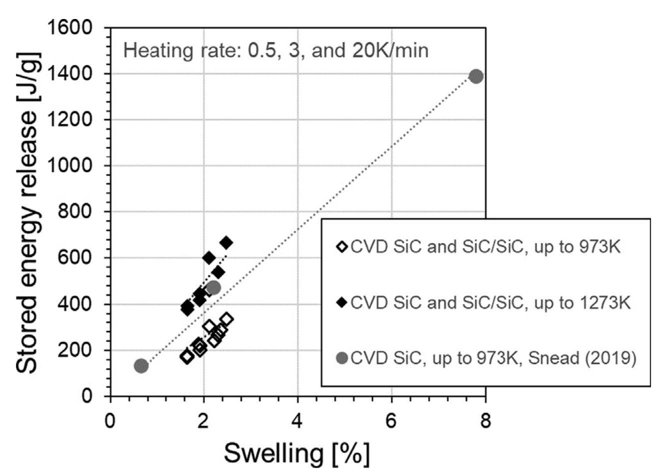


**Fig. 6.** Correlation between stored energy and irradiation-induced swelling of CVD SiC and SiC/SiC composites irradiated at 510–520 K. Literature data for CVD SiC irradiated at $\sim$ 330 K are also plotted [10]. The dotted trend lines are drawn by a linear fit with an intercept at the origin.

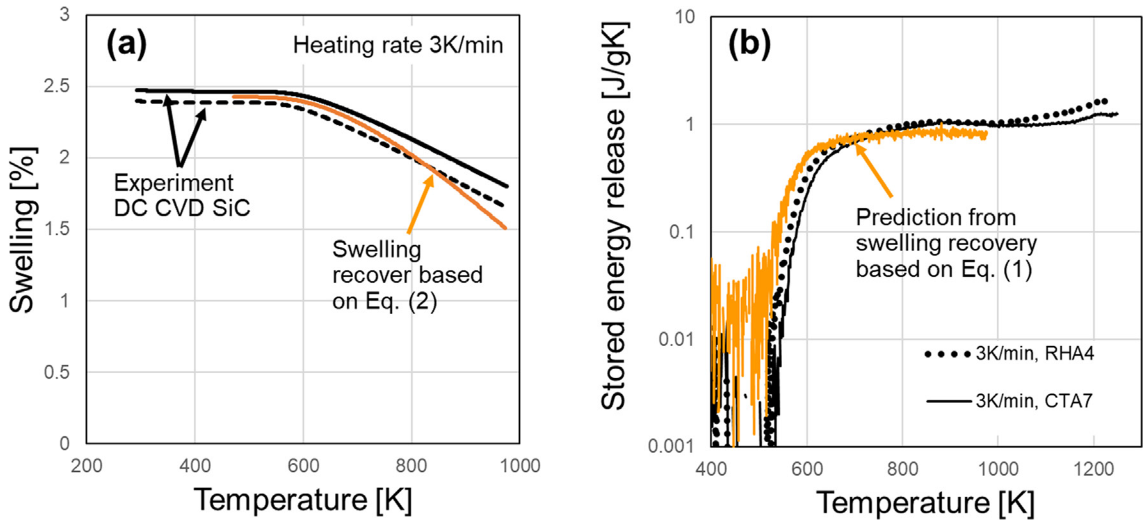


**Fig. 7.** (a) Recovery of swelling of DC CVD SiC upon annealing and (b) energy release of DC and CT CVD SiC. All the specimens were irradiated at ~ 500 K to 2 dpa. The heating rate of the annealing was 3 K/min for both swelling and energy release data. Model predictions of swelling recovery and energy release are also shown.

$$\tau(T) = \tau_0 \exp(\frac{E_a}{kT}) \quad (5)$$

where $\tau_0$ is a pre-exponential factor proportional to the Debye frequency, $E_a$ is the activation energy or energy barrier for recombination of Frenkel pairs, and $k$ is the Boltzmann constant. It is likely that the recovery stage cannot be determined by single $E_a$; the activation energy for SiC gradually increases with increasing annealing temperature, and the defect recovery does not show a clear recovery stage [33]. This is because irradiation induces various types of defects, including vacancies, interstitials, and antisites of silicon and carbon, and clusters of these defects. It is expected that different swelling recovery mechanisms govern at different temperatures. Even at the same temperature, multiple activation energies of defect recovery have been reported for SiC, and the presence of two energy barriers for recovery has been suggested in the literature [33]. Therefore, this study obtained $\tau(T)$ from the DSC curves; each DSC curve during heating could provide $\tau(T)$ based on Eq. (2) since the only unknown parameter is $\tau(T)$. Fig. 8 shows $\tau(T)$ plotted against the reciprocal temperature. Averaged DSC curves for each heating rate were used for the analysis. Note that the 0.5 K/min curves could not provide $\tau(T)$ because the data fluctuation made the analysis challenging. As was expected because multiple defect recovery mechanisms were involved, Eq. (5) cannot describe $\tau(T)$ with a single activation energy. In addition, $\tau(T)$ depends on the heating rate, suggesting that the initial microstructure affects the decay behavior of swelling and energy release. A description of $\tau(T)$ for each heating rate was obtained as follows, and the trend lines are shown in Fig. 8.

$$\tau(T) = \tau_1 \exp\left(\frac{T_1}{T}\right) + \tau_2 \exp(\frac{T_2}{T}) \quad (6)$$

The fitting parameters are $\tau_1$ = 8.00 × $10^{-5}$ [s], $\tau_2$ = 3.15 × $10^2$ [s], $T_1$ = 1.10 × $10^4$ [K], and $T_2$ = 7.74 × $10^2$ [K] for the heating rate of 20 K/min and $\tau_1$ = 2.00 × $10^{-5}$ [s], $\tau_2$ = 1.05 × $10^3$ [s], $T_1$ = 1.1 0 × $10^4$ [K], and $T_2$ = 7.74 × $10^2$ [K] for 3 K/min. The fitting was aimed at descriptions of the low-temperature regime (<973 K) because $\tau(T)$ is dependent on material type, as seen in the energy release behavior in Fig. 4. Fig. 8 also shows the expected trend line for the 0.5 K/min case. The fitting parameters of $\tau_1$ = 2.00 × $10^{-5}$ [s], $\tau_2$ = 5.00 × $10^3$ [s], $T_1$ = 1.10 × $10^4$ [K], and $T_2$ = 7.74 × $10^2$ [K] for the heating rate 0.5 K/min were found to describe the experimental data as explained below.

Based on Eqs. (1), (2), (3), and (6), the energy release curve was reproduced and compared with the experimental data as shown in Fig. 9. The model lines describe the experimental data well, especially for the early stage of energy release. This is because $\tau(T)$ was obtained from the energy release curves. Therefore, Fig. 9 does not necessarily validate the equations. Especially for the 0.5 K/min case, the parameters in Eq. (6) were set to describe the experimental results.

Validation of the model was attempted by a comparison of the model and experimental results independently obtained. Fig. 7a compares the swelling recovery behavior of the dilatometry experiment with a 3 K/min heating rate, and the predication from the swelling recovery model (Eq. [2]). The model describes the trend up to 800 K, consistent with the good agreement of the energy release curve and the model at low temperatures in Fig. 9. Validation of the stored energy–swelling conversion constant, $k$ = 4.25 × $10^4$ (J/g), can be assessed based on the energetics of radiation defects in SiC. In a previous study, Snead et al. discussed stored energy in neutron-irradiated SiC based on the formation energy

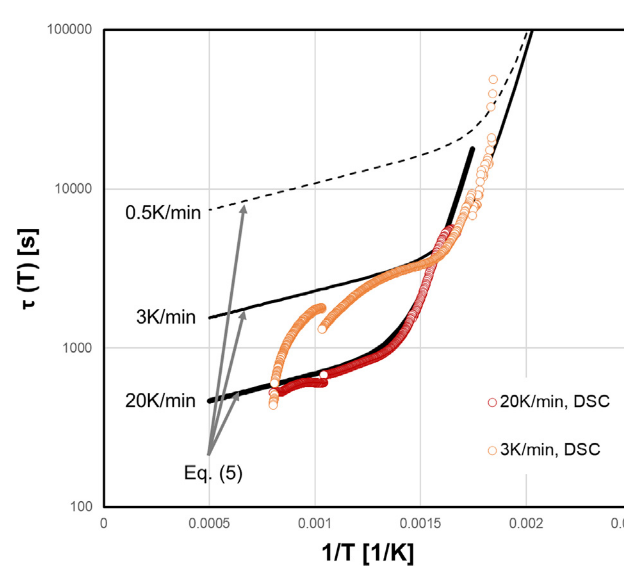


**Fig. 8.** Lifetime of recovery of radiation defects, $\tau(T)$, as a function of temperature for heating rates of 20 and 3 K/min.

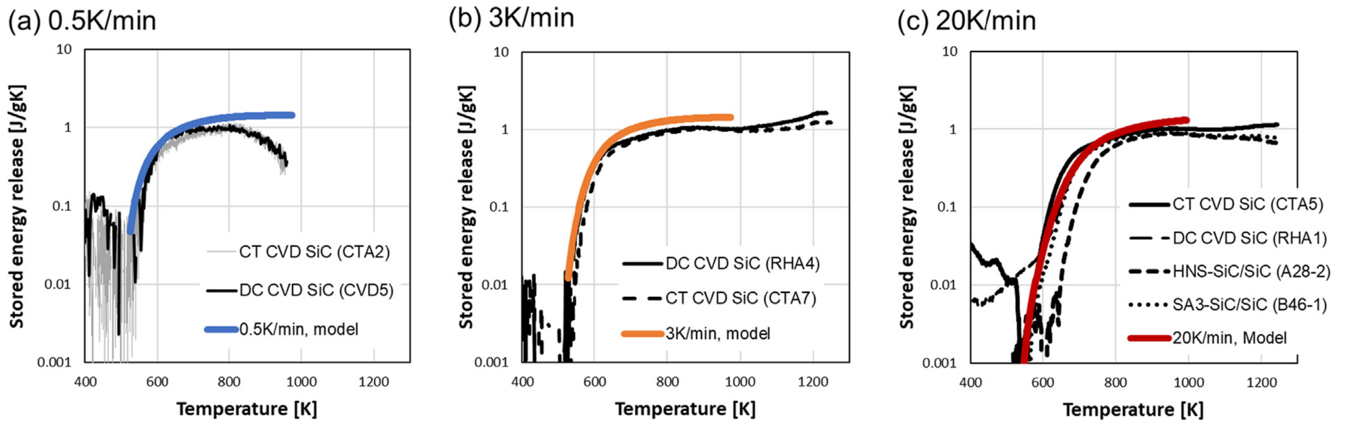


**Fig. 9.** Comparison of experimental and modeled energy release under DSC experiment with different heating rates: (a) 0.5 K/min, (b) 3 K/min, and (c) 20 K/min. The experimental curves are in grayscale, and the modeled curves are in colors.

of point defects (interstitial, monovacancies, and antisites of silicon and carbon [six types in all]) [10] and estimated 293 J/g at 1 % swelling ($k$ = 2.93 × $10^4$ (J/g)) for the case of irradiation at ~ 330 K. At the irradiation temperature of ~ 500 K in this study, the point defect assumption could still be valid because it is within the point defect swelling regime of SiC, in which vacancies are practically immobile and act as effective sinks for interstitials to prevent large clustering [9]. Therefore, the finding that the stored energy–swelling conversion between the experiment and the calculation are of the same order of magnitude encourages the use of the model proposed in this study.

The most direct approach to assessing the reliability of Eq. (1) is to compare the modeled and experimental energy release behavior during isothermal annealing. Each DSC signal was recorded at the maximum test temperature for at least 30 min, as shown in Table 1. The DSC signals (in volts) were converted to heat generation (in watts) based on a correlation factor obtained from a sapphire standard specimen to calculate the amount of energy released. Fig. 10 shows the energy release rate during the isothermal runs at 673 and 973 K, along with the predicted values based on Eq. (1). The results for 1,273 K are not shown because Eq. (1) is not intended to model behavior at this temperature. For both temperatures, agreement was obtained regarding the order of magnitude of the initial energy release rate between the experiment and the model. The consistency at the initial annealing stage is important in modeling the energy release rate during heating, especially for high heating rate of 20 K/min, because of the relevance of the time scale. In addition, the model qualitatively captures the decrease of the energy release rate from 673 to 973 K, although a discrepancy in the absolute values can be seen after hundreds of annealing runs. The discrepancy could be explained by the operation of multiple recovery mechanisms; swelling recovery studies indicated the presence of two energy barriers for defect recovery at a constant temperature [33]. Because Eq. (6) considers only the initial recovery stage, it is possible that Eq. (2) does not predict the long-term annealing behavior. In summary, the swelling recovery model was able to explain the energy release behavior. Future research opportunity exists to build a theoretical equation for $\tau(T)$, rather than using the empirical equation.

It is worth mentioning that the method used to build the mechanistic model, Eq. (1), is unique and different from the one applied to graphite, the stored energy of which has extensively been studied. Graphite exhibited well-defined peaks of energy release rates upon a linear rise in temperature under certain irradiation conditions, allowing the interpretation of the rate of energy release

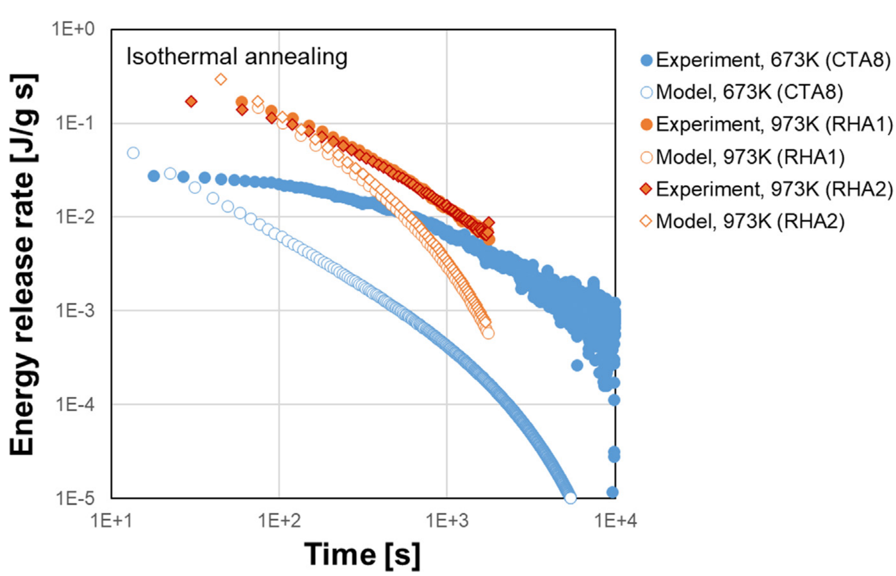


**Fig. 10.** Energy release rate during isothermal annealing of irradiated CVD SiC materials. The model prediction results based on Eq. (2) are also presented.

based on relatively simple Arrhenius equations [34]. Such information aids the understanding of the energy release of graphite in the absence of a clear recovery stage [35]. However, SiC did not show a sharp energy release peak, as shown in Fig. 4 and Fig. 5. Even in the case of the 0.5 K/min heating rate, the peak at 800 K was broad and thus could consist of multiple peaks. It is understandable that SiC exhibited more complex recovery behavior compared with graphite because SiC, a binary system, could have various types of defect clusters with different stoichiometries, which is not the case for graphite. Therefore, this study modeled the energy release behavior on the swelling–energy release correlation rather than by identifying each defect recombination mechanism. This modeling was achieved by acknowledging the established irradiation-induced swelling mechanisms and studies of defect recovery under various annealing conditions [9].

The linear relationship between stored energy release and swelling recovery (Eq. [1]) also enables the explanation of underlying mechanisms of the energy release process. Electron microscopy analysis [36] revealed that atomistic radiation defects, which are expected to be dominant in the irradiation temperatures used in this study [9], are responsible for irradiation-induced swelling of SiC; previous studies of neutron-irradiated SiC (same grade of DC CVD SiC) revealed the presence of tri-vacancy clusters following irradiation at 650 K at 0.11 and 1.5 dpa by positron annihilation spectroscopy [37], and multiple vacancy, antisite, and atomistic defect clusters were determined by high-energy x-ray diffraction analysis [38]. Recovery of radiation defects upon annealing in β-SiC irradiated at temperatures below 423 K has three stages: stage I at 423 K, stage II at 623 K, and stage III at 1,023 K, which are driven by mobilities of C interstitial, Si interstitial, and Si vacancy, respectively [39,40]. These recovery stages were absent in the DSC curves because of the multimodal defect recovery process involving a point defect recombination barrier [41], recovery of various types of defects with different size and stoichiometry [42], transformation of a defect complex (e.g., decrease in Si vacancy color center above 700 °C [43,44]), and reclustering of self-interstitial atoms during recovery [45]. Therefore, the transition temperatures of the recovery stages II and III likely change mechanisms of the stored energy release, although the transition is not clear in the DSC curves because of the absence of a dominant defect recovery reaction.

### 4.2. Material-dependent energy release behavior

The energy release behavior is material-dependent at > 1,000 K, at which both silicon and carbon interstitials are effectively mobile [9]. Under the circumstances, defect sinks such as grain boundaries and stacking faults, which are common processing defects in SiC, in the CVD SiC and SiC/SiC composites and phase boundaries in the SiC/SiC composites could play an important role in defect recovery and thus in energy release. This hypothesis is supported by a computer simulation study by Jiang et al. reporting small tilt grain boundaries as effective sinks of interstitials at > 873 K [46]. This effect could be operational in HNS and SA3 SiC fibers with typical grain sizes less than ~ 200 nm [47]. Ishimaru et al. reported that high-density stacking faults with a similar appearance to those in Fig. 1b were the origin of resistance to radiation-induced amorphization of SiC because of point defect migrations confined between the planar defects [48]; this finding also supports material-dependent energy release. This is consistent with effective annihilation of radiation defects at grain boundaries found in nanostructured materials [49]. The carbon interphase in the composites and carbon secondary phases in HNS and SA3 fibers [47] could also affect the stored energy. The SiC/C phase boundaries are expected to exhibit irradiation-induced inter-atomic diffusion, a defect which is absent in pure SiC [50]. However, the effects of carbon phases are not expected to be dominant because of the limited volume fraction (<5 vol% in total). Material dependence is also expected at higher temperatures, which this study did not investigate via DSC. Differential swelling recovery behavior between high-purity monolithic SiC and SA3-CVI SiC/SiC composites was reported at > 1,473 K [51], suggesting different energy release behaviors among the monolithic and composite materials. The difference in displacements per atom damage between the CVD SiC and SiC/SIC composites is not expected to affect the energy release because in both cases, swelling was beyond the expected neutron damage needed to reach saturated swelling [9]. To understand material-dependent energy release, additional experiments with higher annealing temperatures will be required in future research.

### 4.3. Implication of the results for accident behavior and future research directions

To the best of our knowledge, this is the first report on the stored energy release behavior of SiC irradiated under LWR-relevant temperatures. In previous studies [10,16], the irradiation temperature (<463 K) was much lower than the LWR coolant temperature (~573 K). Therefore, the previous studies did not provide clear insight into energy release in SiC under LWR accident conditions. Based on the energy release behavior of the SiC/SiC composites at a 20 K/min heating rate relevant to a heating rate during a station blackout accident [52], the rate of energy release does not exceed the specific heat capacity up to 1,273 K; that is a positive finding for LWR applications, albeit it is necessary to understand why the energy release exceeds the specific heat capacity in CVD SiC at the 3 K/min heating rate (RHA4 in Fig. 5). In addition, application irradiation temperatures will be higher than the irradiation temperature used in this study; thus, lower amounts of stored energy are expected in reactor operating conditions, considering the negative temperature dependence of swelling of SiC (Eq. [4]). The significant energy release from the RHA4 may be caused by the larger number of irradiation defects before annealing rather than the heating rate effect based on the correlation between swelling and stored energy released (Fig. 6).

To determine the stored energy release of irradiated SiC, additional DSC runs at higher temperatures are required because only part of the stored energy was likely released at temperatures of up to 1,273 K, which was the highest test temperature of this study. The fraction of the stored energy released was estimated based on the swelling–stored energy conversion ($k$ = 4.25 $\times$ $10^4$ [J/g]), DSC results, and irradiation-induced swelling. The specimens irradiated at 510–520 K and 880 K experienced 51%–67% and 24% energy releases, respectively, up to 1,273 K. This result suggests concerns regarding the energy release at > 1,273 K in applications if the energy release occurs rapidly. Previous studies on recovery of irradiation defects in SiC reported that an annealing temperature of at least 1,673 K is required to remove defects by annealing [51]. Temperatures at that level will be required for DSC experiments to study energy release. The maximum temperature of the DSC test in this study was limited by the instrument capability. The instrument needs include ensuring the chemical compatibility of the pan and test specimens. A Pt/Rh pan is expected to undergo a chemical reaction with SiC at 1,673 K. Alternative materials for the pan could be alumina and graphite. Chemical compatibility may not be an issue, but these materials are less sensitive to heat capacity measurements during DSC than Pt/Rh. Future research also necessitates DSC tests with higher heating rates to understand the energy release behavior under specific accident conditions (e.g., large break loss of a coolant accident with a heating rate of > 500 K/min [53]).

A potential approach to studying energy release under extreme temperatures is to utilize the correlation between stored energy and swelling. It is reasonable to expect that Eq. (1) describes the entire energy release behavior, considering defect recombination as a source of energy release regardless of temperature. If that is true, dilatometry runs at elevated temperatures will indirectly provide insights into the energy release. Dilatometry of a SiC specimen is relatively easier than DSC runs because dilatometry is a precise method regardless of temperature, and chemical compatibility between the specimen and the fixture is less critical because the area of contact between the specimen and the fixture is limited in dilatometry. Dilatometry of high-temperature ceramics has been demonstrated at temperatures up to 2,273 K [23]. The previous studies of swelling recovery in SiC found gradual defect recovery in SiC and no clear recovery stage up to 1,673 K [51]. These findings suggest the absence of a sharp energy release peak in the DSC curve of irradiated SiC at > 1,273 K, which needs to be confirmed in future research. Nevertheless, the energy release model built in this study will be useful to assessing the safety of LWR core structures at the beginning of accidents up to $\sim$ 973 K. This assessment is crucial because the stored energy release rapidly increases from the onset temperature as shown in Fig. 4 and Fig. 5 and consequently changes the thermo-mechanical properties and dimensions (swelling recovery and thermal expansion) of the SiC structure. Additionally, the large amount of stored energy in SiC could produce a new application of SiC material to an energy storage system by defect engineering. The swelling-stored energy conversion, $k$, predicts a total stored energy up to 1,020 J/g for the CVD 5 specimen. The largest stored energy reported for irradiated SiC was $\sim$ 2,500 J/g for neutron irradiation at 330 K to $\sim$ 1 dpa, inferred from the dose-dependent stored energy [10]. The amount is in the same order as that of Li ion batteries ($\sim$1,800 J/g [54]). Recently, stored energy of irradiated graphite was proposed for a new energy storage system [55,56]. Considering the same order of magnitude of gravimetric energy density between irradiated SiC and graphite [55], SiC could alternate the graphite component proposed because of the superior oxidation resistance of SiC compared with graphite. The energy release model of this study will help in designing the energy conversion process. In summary, stored energy release in irradiated SiC has two aspects: risks of stored energy release in nuclear reactor applications and the potential for energy storage applications.

## 5. Conclusions

This study investigated the stored energy release in monolithic and SiC/SiC composites that were neutron-irradiated at 510–520 K or 880 K to $\sim$ 2 or 12 dpa by DSC with different heating rates. To the best of our knowledge, this is the first study providing insights into the stored energy release behavior of SiC during LWR accidents by using relevant test specimens. The findings can be summarized as follows. The energy release behavior was affected by the heating rate; the onset of energy release was delayed, and the energy release at the beginning became gradual with an increase in the heating rate from 0.5 to 20 K/min. The microstructures of the unirradiated materials (e.g., CVD SiC vs. SiC/SiC) did not have a notable effect on the energy release up to $\sim$ 973 K but did have an effect beyond that temperature.

This study proposed a mechanistic model of the stored energy release (Eq. [1]) assuming a linear relationship between the stored energy release rate and the swelling recovery rate. The model was valid up to 973 K, at which the energy release behavior was independent of the material type. The analysis indicated a linear conversion factor of swelling to an energy release of $4.25 \times 10^4$ J/g (425 J/g per 1% of volumetric swelling). The mechanistic model suggested that approximately half of the energy was still stored in the specimens after annealing at 1,273 K in the case of irradiation at 500 K. To conclude the stored energy release model, a theoretical equation for $\tau(T)$ must be built, rather than using the empirical equation. Nevertheless, the energy release model is useful for designing safety feature of SiC structure under the modeling response of SiC-based core structures to early accident conditions in which the rapid energy release continuously changes thermo-mechanical properties and dimensions of SiC structures and could increase the temperature of a fuel assembly and cause fuel-clad contact. Additionally, the significant amount of energy stored in irradiated SiC could create new development opportunities of energy storage materials by defect engineering. The energy release model will be useful for designing the energy conversion process.

## Declaration of Competing Interest

The authors declare that they have no known competing financial interests or personal relationships that could have appeared to influence the work reported in this paper.

## Acknowledgments

This study was supported by the US Department Energy (DOE), Office of Nuclear Energy, for the Advanced Fuels Campaign of the Nuclear Technology R&D program and the Westinghouse Electric Corporation/General Atomics FOA program under contact DE-AC05-00OR22725 with ORNL, managed by UT Battelle, LLC. Irradiation experiments on CVD SiC specimens were supported by the DOE Office of Fusion Energy Sciences under contract DE-AC05-00OR22725, and by IMR Tohoku University under contract NFE-13-04416 with UT-Battelle, LLC. A portion of this research used resources at the HFIR, a DOE Office of Science User Facility operated by ORNL. Stephanie Curlin at ORNL contributed to the DSC experiments. The authors wish to thank Peter Doyle, Anne Campbell, and Olivia Shafer at ORNL for reviewing and editing this manuscript.

## References

[1] B. Almutairi, S. Jaradat, D. Kumar, C.S. Goodwin, S. Usman, A. Alajo, S.B. Alam, Weight loss and burst testing investigations of sintered silicon carbide under oxidizing environments for next generation accident tolerant fuels for SMR applications, Mater. Today Commun. 30 (2022) 102958, https://doi.org/10.1016/j.mtcomm.2021.102958.

[2] J. Braun, C. Sauder, J. Lamon, F. Balbaud-Célérier, Influence of an original manufacturing process on the properties and microstructure of SiC/SiC tubular composites, Compos. Part A Appl. Sci. Manuf. 123 (2019) 170–179, https://doi.org/10.1016/j.compositesa.2019.04.031.

[3] J. Nance, G. Subhash, B. Sankar, R. Haftka, N.H. Kim, C. Deck, S. Oswald, Measurement of Residual Stress in Silicon Carbide Fibers of Tubular Composites Using Raman Spectroscopy, Acta Mater. 217 (2021) 117164, https://doi.org/10.1016/j.actamat.2021.117164.

[4] X.i. Liu, R. Wang, D. Hu, L. Zhang, G. Chen, Degradation analysis on high-cycle bending fatigue for woven SiC/SiC composites based on Wiener process model, Mater. Des. 198 (2021) 109295, https://doi.org/10.1016/j.matdes.2020.109295.

[5] Y. Ikarashi, T. Ogasawara, T. Aoki, Effects of cyclic tensile loading on the rupture behavior of orthogonal 3-D woven SiC fiber/SiC matrix composites at elevated temperatures in air, J. Eur. Ceram. Soc. 39 (4) (2019) 806–812, https://doi.org/10.1016/j.jeurceramsoc.2018.10.016.

[6] Y. Ikarashi, T. Ogasawara, T. Aoki, Micromechanical model of time-dependent damage and deformation behavior for an orthogonal 3D-woven SiC/SiC composite at elevated temperature in vacuum, J. Eur. Ceram. Soc. 40 (12) (2020) 3887–3896, https://doi.org/10.1016/j.jeurceramsoc.2020.04.029.

[7] Z. Peng, X. Wang, Z. Wu, A bundle-based shear-lag model for tensile failure prediction of unidirectional fiber-reinforced polymer composites, Mater. Des. 196 (2020) 109103, https://doi.org/10.1016/j.matdes.2020.109103.

[8] A.A. Campbell, W.D. Porter, Y. Katoh, L.L. Snead, Method for analyzing passive silicon carbide thermometry with a continuous dilatometer to determine irradiation temperature, Nucl. Instruments Methods Phys. Res. Sect. B Beam Interact. with Mater. Atoms. 370 (2016) 49–58, https://doi.org/10.1016/j.nimb.2016.01.005.

[9] L.L. Snead, T. Nozawa, Y. Katoh, T.-S. Byun, S. Kondo, D.A. Petti, Handbook of SiC properties for fuel performance modeling, J. Nucl. Mater. 371 (1-3) (2007) 329–377, https://doi.org/10.1016/j.jnucmat.2007.05.016.

[10] L.L. Snead, Y. Katoh, T. Koyanagi, K. Terrani, Stored energy release in neutron irradiated silicon carbide, J. Nucl. Mater. 514 (2019) 181–188, https://doi.org/10.1016/j.jnucmat.2018.12.005.
[11] R. Krishna, J. Wade, A.N. Jones, M. Lasithiotakis, P.M. Mummery, B.J. Marsden, An understanding of lattice strain, defects and disorder in nuclear graphite, Carbon N. Y. 124 (2017) 314–333, https://doi.org/10.1016/j.carbon.2017.08.070.
[12] C.P. Ewels, R.H. Telling, A.A. El-Barbary, M.I. Heggie, P.R. Briddon, Metastable Frenkel Pair Defect in Graphite: Source of Wigner Energy?, Phys Rev. Lett. 91 (2003), https://doi.org/10.1103/PhysRevLett.91.025505 025505.
[13] A.A. Campbell, T.D. Burchell, Radiation Effects in Graphite, in: Compr. Nucl. Mater., Elsevier, 2020: pp. 398–436. doi:10.1016/B978-0-12-803581-8.12055-7.
[14] C. Sauder, Ceramic Matrix Composites: Nuclear Applications, in, Ceram. Matrix Compos. Mater. Model. Technol. (2014) 609–646, https://doi.org/10.1002/9781118832998.ch22.
[15] W. Li, K. Shirvan, S. Harrison, J. Pegna, Innovative accident tolerant fuel concept enabled through direct manufacturing technology, Appl. Energy. 264 (2020) 114742, https://doi.org/10.1016/j.apenergy.2020.114742.
[16] W. Primak, L.H. Fuchs, P.P. Day, Radiation damage in diamond and silicon carbide, Phys. Rev. 103 (5) (1956) 1184–1192, https://doi.org/10.1103/PhysRev.103.1184.
[17] M.N. Mirzayev, B.A. Abdurakhimov, E. Demir, A.A. Donkov, E. Popov, M.Y. Tashmetov, I.G. Genov, T.T. Thabethe, K. Siemek, K. Krezhov, F. Mamedov, D.M. Mirzayeva, M.V. Bulavin, V.A. Turchenko, T.X. Thang, T.Z. Abdurakhmonov, P. Horodek, Investigation of the formation of defects under fast neutrons and gamma irradiation in 3C–SiC nano powder, Phys. B Condens. Matter. 611 (2021) 412842, https://doi.org/10.1016/j.physb:2021.412842.
[18] M.J. Madito, T.T. Hlatshwayo, C.B. Mtshali, Chemical disorder of a-SiC layer induced in 6H-SiC by Cs and I ions co-implantation: Raman spectroscopy analysis, Appl. Surf. Sci. 538 (2021) 148099, https://doi.org/10.1016/j.apsusc.2020.148099.
[19] C. Kasper, D. Klenkert, Z. Shang, D. Simin, A. Gottscholl, A. Sperlich, H. Kraus, C. Schneider, S. Zhou, M. Trupke, W. Kada, T. Ohshima, V. Dyakonov, G.V. Astakhov, Influence of Irradiation on Defect Spin Coherence in Silicon Carbide, Phys. Rev. Appl. 13 (2020), https://doi.org/10.1103/PhysRevApplied.13.044054 044054.
[20] S. Khani Moghanaki, M. Kazeminezhad, R. Logé, Recrystallization behavior of multi-directionally forged over-aged and solution treated Al-Cu-Mg alloy during non-isothermal annealing, Mater. Des. 132 (2017) 250–256, https://doi.org/10.1016/j.matdes.2017.07.011.
[21] Y.-B. Ma, B.-Z. Wang, Q.-D. Zhang, Y. Jiang, D.-W. Hou, X. Cui, F.-Q. Zu, Change dynamic behaviors by heightening its stored energy of monolithic bulk metallic glass, Mater. Des. 181 (2019) 107971, https://doi.org/10.1016/j.matdes.2019.107971.
[22] N. Sohrabi, J. Jhabvala, G. Kurtuldu, M. Stoica, A. Parrilli, S. Berns, E. Polatidis, S. Van Petegem, S. Hugon, A. Neels, J.F. Löffler, R.E. Logé, Characterization, mechanical properties and dimensional accuracy of a Zr-based bulk metallic glass manufactured via laser powder-bed fusion, Mater. Des. 199 (2021) 109400, https://doi.org/10.1016/j.matdes.2020.109400.
[23] E. Zapata-Solvas, D.D. Jayaseelan, P.M. Brown, W.E. Lee, Thermal properties of La2O3-doped ZrB2- and HfB2-based ultra-high temperature ceramics, J. Eur. Ceram. Soc. 33 (15-16) (2013) 3467–3472, https://doi.org/10.1016/j.jeurceramsoc.2013.06.009.
[24] ASTM International, Standard Test Method for Determining Specific Heat Capacity by Differential Scanning Calorimetry, in: 2018: p. ASTM E1269-11. doi:10.1520/E1269-11R18.
[25] L. Charpentier, M. Balat-Pichelin, H. Glénat, E. Bêche, E. Laborde, F. Audubert, High temperature oxidation of SiC under helium with low-pressure oxygen. Part 2: CVD β-SiC, J. Eur. Ceram. Soc. 30 (12) (2010) 2661–2670, https://doi.org/10.1016/j.jeurceramsoc.2010.04.031.
[26] Y. Yamamoto, Y. Murakami, H. Yamaguchi, T. Yamamoto, D. Yonetsu, K. Noborio, S. Konishi, Re-evaluation of SiC permeation coefficients at high temperatures, Fusion Eng. Des. 109–111 (2016) 1286–1290, https://doi.org/10.1016/j.fusengdes.2015.12.041.
[27] H.L. Heinisch, L.R. Greenwood, W.J. Weber, R.E. Williford, Displacement damage in silicon carbide irradiated in fission reactors, J. Nucl. Mater. 327 (2-3) (2004) 175–181, https://doi.org/10.1016/j.jnucmat.2004.02.012.
[28] R. Karsthof, M.E. Bathen, A. Galeckas, L. Vines, Conversion pathways of primary defects by annealing in proton-irradiated n-type 4H-SiC, Phys. Rev. B. 102 (2020), https://doi.org/10.1103/PhysRevB.102.184111 184111.
[29] W.J. Weber, W. Jiang, S. Thevuthasan, Defect annealing kinetics in irradiated 6H–SiC, Nucl. Instruments Methods Phys. Res. Sect. B Beam Interact. with Mater. Atoms. 166–167 (2000) 410–414, https://doi.org/10.1016/S0168-583X(99)00868-X.
[30] F. Gao, W.J. Weber, Recovery of close Frenkel pairs produced by low energy recoils in SiC, J. Appl. Phys. 94 (7) (2003) 4348–4356, https://doi.org/10.1063/1.1605254.
[31] T. Koyanagi, T. Nozawa, Y. Katoh, L.L. Snead, Mechanical property degradation of high crystalline SiC fiber–reinforced SiC matrix composite neutron irradiated to ~100 displacements per atom, J. Eur. Ceram. Soc. 38 (4) (2018) 1087–1094.
[32] Y. Katoh, T. Koyanagi, J.L. McDuffee, L.L. Snead, K. Yueh, Dimensional stability and anisotropy of SiC and SiC-based composites in transition swelling regime, J. Nucl. Mater. 499 (2018) 471–479, https://doi.org/10.1016/j.jnucmat.2017.12.009.
[33] T. Yano, Y. You, K. Kanazawa, T. Kobayashi, M. Imai, K. Yoshida, S. Yamazaki, Recovery behavior of neutron-irradiation-induced point defects of high-purity β-SiC, J. Nucl. Mater. 455 (1-3) (2014) 445–449, https://doi.org/10.1016/j.jnucmat.2014.07.068.
[34] R.H. Telling, M.I. Heggie, Radiation defects in graphite, Philos. Mag. 87 (31) (2007) 4797–4846, https://doi.org/10.1080/14786430701210023.
[35] R. Mittal, M.K. Gupta, S.K. Mishra, S. Wajhal, H.K. Poswal, B. Singh, A.B. Shinde, P.S.R. Krishna, P.D. Babu, R. Mishra, P.U. Sastry, R. Ranjan, S.L. Chaplot, Defect topology and annihilation by cooperative movement of atoms in neutron-irradiated graphite, Phys. Rev. B. 102 (2020), https://doi.org/10.1103/PhysRevB.102.064103 064103.
[36] S. Yang, Y. Nakagawa, M. Kondo, T. Shibayama, Electron energy-loss spectroscopic evaluation of depth-dependent swelling of He + ion-irradiated 4H-SiC correlated with defect type, J. Appl. Phys. 127 (17) (2020) 175106, https://doi.org/10.1063/1.5143399.
[37] X. Hu, T. Koyanagi, Y. Katoh, B.D. Wirth, Positron annihilation spectroscopy investigation of vacancy defects in neutron-irradiated 3C-SiC, Phys. Rev. B. 95 (2017), https://doi.org/10.1103/PhysRevB.95.104103.
[38] D.J. Sprouster, T. Koyanagi, E. Dooryhee, S.K. Ghose, Y. Katoh, L.E. Ecker, Microstructural evolution of neutron irradiated 3C-SiC, Scr. Mater. 137 (2017) 132–136, https://doi.org/10.1016/j.scriptamat.2017.02.030.
[39] H. Itoh, N. Hayakawa, I. Nashiyama, E. Sakuma, Electron spin resonance in electron-irradiated 3C-SiC, J. Appl. Phys. 66 (9) (1989) 4529–4531, https://doi.org/10.1063/1.343920.
[40] F. Gao, W.J. Weber, M. Posselt, V. Belko, Atomistic study of intrinsic defect migration in 3C-SiC, Phys. Rev. B. 69 (2004), https://doi.org/10.1103/PhysRevB.69.245205 245205.
[41] M.J. Zheng, N. Swaminathan, D. Morgan, I. Szlufarska, Energy barriers for point-defect reactions in 3C-SiC, Phys. Rev. B - Condens. Matter Mater. Phys. 88 (2013), https://doi.org/10.1103/PhysRevB.88.054105.
[42] G. Bonny, L. Buongiorno, A. Bakaev, N. Castin, Models and regressions to describe primary damage in silicon carbide, Sci. Rep. 10 (2020) 10483, https://doi.org/10.1038/s41598-020-67070-x.
[43] H.J. von Bardeleben, E. Rauls, U. Gerstmann, Carbon vacancy-related centers in 3C-silicon carbide: Negative-U properties and structural transformation, Phys. Rev. B. 101 (2020), https://doi.org/10.1103/PhysRevB.101.184108 184108.
[44] Y. Fan, Y. Song, Z. Xu, B. Dong, J. Wu, M. Rommel, K. Zhang, J. Zhao, R. Zhu, B. Li, Q. Li, F. Fang, Molecular dynamics simulation of color centers in silicon carbide by helium and dual ion implantation and subsequent annealing, Ceram. Int. 47 (17) (2021) 24534–24544, https://doi.org/10.1016/j.ceramint.2021.05.172.
[45] P.F. Wang, Y.F. Ruan, L. Huang, W. Zhu, Nitrogen-promoted formation of graphite-like aggregations in SiC during neutron irradiation, J. Appl. Phys. 111 (6) (2012) 063517, https://doi.org/10.1063/1.3697681.
[46] H. Jiang, X. Wang, I. Szlufarska, The Multiple Roles of Small-Angle Tilt Grain Boundaries in Annihilating Radiation Damage in SiC, Sci. Rep. 7 (2017) 42358, https://doi.org/10.1038/srep42358.
[47] J.A. DiCarlo, H.-M. Yun, Non-oxide (Silicon Carbide) Fibers, in: Handb. Ceram. Compos., Springer US, 2005: pp. 33–52. doi:10.1007/0-387-23986-3_2.
[48] M. Ishimaru, Y. Zhang, S. Shannon, W.J. Weber, Origin of radiation tolerance in 3C-SiC with nanolayered planar defects, Appl. Phys. Lett. 103 (3) (2013) 033104, https://doi.org/10.1063/1.4813593.
[49] M. Wurmshuber, D. Frazer, A. Bachmaier, Y. Wang, P. Hosemann, D. Kiener, Impact of interfaces on the radiation response and underlying defect recovery mechanisms in nanostructured Cu-Fe-Ag, Mater. Des. 160 (2018) 1148–1157, https://doi.org/10.1016/j.matdes.2018.11.007.
[50] J. Du, Y. Huang, J. Liu, Y. Liu, Z. Wang, Irradiation damage alloying for immiscible alloy systems and its thermodynamic origin, Mater. Des. 170 (2019) 107699, https://doi.org/10.1016/j.matdes.2019.107699.
[51] M.I. Idris, S. Yamazaki, K. Yoshida, T. Yano, Recovery behavior of SiC f /SiC composites by post-irradiation annealing up to of 1673 K, Energy Procedia. 131 (2017) 413–419, https://doi.org/10.1016/j.egypro.2017.09.461.
[52] S. Liu, R. Liu, C. Qiu, W. Zhou, Multiphysics Modeling of Thorium-Based Fuel Performance With Cr-Coated SiC/SiC Composite Under Normal and Accident Conditions, Front. Energy Res. 9 (2021), https://doi.org/10.3389/fenrg.2021.677606.
[53] S.W. Lee, H.T. Kim, I.C. Bang, Performance evaluation of UO2/graphene composite fuel and SiC cladding during LBLOCA using MARS-KS, Nucl. Eng. Des. 257 (2013) 139–145, https://doi.org/10.1016/j.nucengdes.2013.01.012.
[54] C. Julien, A. Mauger, A. Vijh, K. Zaghib, Lithium Batteries, in: Lithium Batter., Springer International Publishing, Cham, 2016, pp. 29–68. doi:10.1007/978-3-319-19108-9_2.
[55] I.-T. Lu, M. Bernardi, Using defects to store energy in materials – a computational study, Sci. Rep. 7 (2017) 3403, https://doi.org/10.1038/s41598-017-01434-8.
[56] R. Ponciroli, N. Stauff, Z.-G. Mei, P. Shriwise, L. Brockmeyer, Y. Cao, B.o. Feng, P. Romano, Integration of a Wigner effect-based energy storage system with an advanced nuclear reactor, Nucl. Eng. Des. 385 (2021) 111521, https://doi.org/10.1016/j.nucengdes.2021.111521.